I. Marzo, J. A. Barrena, A. Sanchez-Ruiz, G. Abad and I. Muguruza, "Reactive Power Limits of Single-Phase and Three-Phase DC-Link VSC STATCOMs under Negative-Sequence Voltage and Current," IECON 2021 – 47th Annual Conference of the IEEE Industrial Electronics Society, 2021, pp. 1-8.

https://doi.org/10.1109/IECON48115.2021.9589147

Reactive Power Limits of Single-Phase and Three-Phase DC-Link VSC STATCOMs under Negative-Sequence Voltage and Current

Iosu Marzo[1*], Jon Andoni Barrena[1], Alain Sanchez-Ruiz[2], Gonzalo Abad[1], and Ignacio Muguruza[1]
[1]Electronics and Computer Science Department, University of Mondragon, Arrasate - Mondragon, Spain
[2]Ingeteam R&D Europe, Zamudio, Spain
[*]e-mail: imarzo@mondragon.edu

***Abstract*—This paper analyzes and compares the reactive power limits of single- and three-phase configured dc-link Voltage Source Converter (VSC) structures for Static Synchronous Compensator (STATCOM) to operate with negative-sequence voltage and current. The three-level Neutral Point Clamped (3L NPC) is used as an example of a three-phase dc-link topology. Likewise, the Cascaded H-Bridge (CHB) is used as a single-phase dc-link case, in both star and delta configurations. Modular Multilevel Converter is also considered as a combination of both dc-link configurations. The conclusions drawn are generic whichever the Power Electronics Building Block (PEBB) used in each VSC structure.**

***Index Terms*—Cascaded H-Bridge (CHB), Modular Multilevel Converter (MMC), negative-sequence, Neutral Point Clamped (NPC), Static Synchronous Compensator (STATCOM), Voltage Source Converter (VSC).**

I. Introduction

Multilevel converters have been widely used grid-connected or motor-connected in both utility [1] and industry applications [2]. The evolution of self-commutated semiconductor devices, accompanied with the emergence of new multilevel Voltage Source Converter (VSC) topologies [3], has made it possible to increase the converter voltage and power ratings. This has permitted the introduction of VSCs in High Power – Medium Voltage (MV) applications; foremost among these is the Static Synchronous Compensator (STATCOM).

The STATCOM using multilevel VSCs is frequently used to facilitate the integration of renewable energy-sources (e.g., wind power plants) [4] or large power consuming loads in mining and metal processing (e.g., arc-furnace loads) [5], by helping to meet the requirements imposed by the power system operator. The typical applications of the STATCOM are the improvement of the power system stability, power factor correction, dynamic regulation of line voltages, active power filtering, mitigation of voltage flicker, unbalanced load compensation, and low-voltage ride-through (LVRT) [6].

Nowadays, the three-level Neutral Point Clamped (3L NPC) [7] is the commercially available standard switching branch for MV levels (3.3 kV to 6.6 kV), and it is commonly used for STATCOM. The current power grid makes it increasingly necessary to count on power equipment with higher voltage and power rating. In order to increase the power ratings, the interconnection of 3L NPC Power Electronics Building Blocks (PEBB) is also a common practice [8]. These structures are usually used in order to increase the power capability when the semiconductor voltage limit is achieved.

Besides common advantages of multilevel VSCs [3], since their scalable attributes, those based on modular structures are considered as one of the most attractive topologies for MV STATCOM applications. Their use may allow even the transformerless connection to the grid with improved power quality [9]. Among modular structures, the Cascaded H-Bridge (CHB) and the Modular Multilevel Converter (MMC) are distinguished [5].

Requirements from grid codes are changing and have started to demand negative-sequence injection capability from the power converters [4]. The unbalanced operation is an issue that the STATCOM must face, either in transmission or in distribution systems [10]. The unbalance may ask the STATCOM to withstand negative-sequence current (i^-) and/or voltage (v^-) [11], or to generate them in order to balance the current and/or the voltage at the point of common coupling (PCC) [12]. The operation under v^- and/or i^- may have different impacts on the converter for STATCOM application.

Negative-sequence components in the ac-side have an influence on the dc-side of the converter. Depending on the VSC structure using, the dc-link can be configured as single- or three-phase. The 3L NPC is an example of a common three-phase dc-link VSC topology, while an important feature in CHBs is that each power cell is fed by single-phase dc-links. For its part, the MMC is composed of both single- and three-phase dc-links.

The aim of this paper is to measure the influence of negative-sequence components in single- and three-phase configured dc-link VSCs. As the purpose of the STATCOM is to give reactive power (Q), the quantification of the impact of v^- and/or i^- is made by means of analyzing the Q limits of the 3L NPC, star- and delta-connected CHBs, and MMC.

II. Single- and Three-Phase DC-Link VSCs

A. Three-Level Neutral Point Clamped converter

The diode clamped multilevel converter, initially proposed in 1981 by Nabae *et al.* in a 3L version [7], was the first multilevel VSC topology employed in large scale. The converter can be generally configured as a 3L, 4L, or 5L topology, but

only the 3L one, commonly known as Neutral Point Clamped (NPC), has found wide application in High Power – Medium Voltage scenarios; e.g., STATCOM application. The 3L NPC structure and the standard PEBB are presented in Fig. 1 (a). The converter phase cluster a is composed of four active switches (S_1 to S_4) with four anti-parallel diodes (D_1 to D_4). The dc input voltage of the converter is split by two equal cascaded dc-link capacitors ($C_{d_1} = C_{d_2}$), providing a floating neutral point Z. The diodes connected to this neutral point are known as clamping diodes (D_{Z_1} and D_{Z_2}). The voltage across each of the dc capacitors is the half of the total three-phase dc-link voltage; in this manner, $V_{C_d}/2$ and $-V_{C_d}/2$ voltages can be synthesized [3].

B. Cascaded H-Bridge converter

The Cascaded H-Bridge (CHB) multilevel converter is composed of multiple units of single-phase power cells, connected in cascade on their ac side [13]. This VSC topology requires isolated dc energy-sources to feed each power cell [9]. Different VSC topologies can be used to build the power cells; e.g., the 2L converter, flying capacitor, T-type or the 3L NPC. If two 3L NPC PEBBs are connected forming an H-bridge, the single-phase 5L neutral point clamped H-bridge (5L NPC/HB) VSC is obtained [8]; which is used in this paper as a CHB power cell topology.

The three phase clusters of the CHB can be connected either in star (YCHB) or in delta (DCHB). The circuit diagrams of both configurations are depicted in Figs. 1 (c) and (d). When employing the YCHB, the phase cluster voltage is the line-to-neutral voltage, and the line-to-line voltage when employing the DCHB. Opposite behavior can be found in terms of current. Another feature to consider is that the DCHB requires a solution to minimize the circulating current inside the delta [5]; i.e., control loops and/or magnetic elements (L_f).

As the ac voltage is proportional to the number of power cells, CHB structures are scalable, and direct power grid-connection is often feasible without a bulky step-up transformer [9]. Besides, due to the multilevel waveform, the number of levels can be easily increased with improved power quality compared to non-modular VSC structures such as the 3L NPC [3].

C. Modular Multilevel Converter

The Modular Multilevel Converter (MMC) is composed of two sets of star-connected CHBs, in which the ac sides of multiple cascaded power cells are interconnected to constitute each phase cluster [14]. By separating the phase cluster into an upper and a lower arm, positive and negative voltage levels are generated at the ac side. Fig. 1 (b) shows the circuit configuration of the MMC. If the same power cell voltage is used, to achieve the same voltage rating in the PCC, the MMC needs twice as many power cells per phase cluster than an equivalent CHB converter [5]. However, the MMC can be built with half-bridge power cells, while the CHB needs full-bridge ones.

Unlike CHB structures, the power cells of the MMC share also a common three-phase dc-link. This configuration gives the currents a way to recirculate; being the control of these currents an specific issue to consider in the MMC [15].

III. Instantaneous Active Power with Negative-Sequence Voltage and Current

Generally speaking, the per-phase ac instantaneous active power (p_{ph}) can be calculated by the inner product of the phase voltage and current [10]:

$$p_{ph}(t) = \bar{P}_{ph} + \tilde{p}_{ph}(t) \quad \text{where} \quad ph = \mathrm{a}, \mathrm{b}, \mathrm{c}. \tag{1}$$

As (1) shows, the resulting power contains both an average ($\bar{P}$) and an oscillating ($\tilde{p}$) term. The later oscillates at twice the power grid frequency (2ω), and considering both positive- and negative-sequence voltage (v^+, v^-) and current components (i^+, i^-), it can be developed as

$$\begin{aligned}\tilde{p}_{ph}(t) = &\underbrace{-\frac{V^+I^+}{2}\cos\left(2\omega t + \delta_v^+ + \theta_i^+ + k\frac{4\pi}{3}\right)}_{\tilde{p}_{ph}^{++}} \\ &\underbrace{-\frac{V^+I^-}{2}\cos\left(2\omega t + \delta_v^+ + \theta_i^-\right)}_{\tilde{p}_{ph}^{+-}} \\ &\underbrace{-\frac{V^-I^+}{2}\cos\left(2\omega t + \delta_v^- + \theta_i^+\right)}_{\tilde{p}_{ph}^{-+}} \\ &\underbrace{-\frac{V^-I^-}{2}\cos\left(2\omega t + \delta_v^- + \theta_i^- - k\frac{4\pi}{3}\right)}_{\tilde{p}_{ph}^{--}}\end{aligned} \tag{2}$$

being $k = 0, -1, 1$ for $ph = \mathrm{a}, \mathrm{b}, \mathrm{c}$, respectively. V^+, V^-, δ_v^+ and δ_v^- denote the converter phase positive- and negative-sequence voltage phasor amplitudes and angles. Likewise, I^+, I^-, θ_i^+ and θ_i^- are the amplitudes and angles of current phasors. Meanwhile, the per-phase average active power in (1) can be derived as

$$\begin{aligned}\bar{P}_{ph} = &\underbrace{\frac{V^+I^+}{2}\cos\left(\delta_v^+ - \theta_i^+\right)}_{\bar{P}_{ph}^{++}} + \underbrace{\frac{V^-I^-}{2}\cos\left(\delta_v^- - \theta_i^-\right)}_{\bar{P}_{ph}^{--}} \\ &+ \underbrace{\frac{V^+I^-}{2}\cos\left(\delta_v^+ - \theta_i^- + k\frac{4\pi}{3}\right)}_{\bar{P}_{ph}^{+-}} \\ &+ \underbrace{\frac{V^-I^+}{2}\cos\left(\delta_v^- - \theta_i^+ - k\frac{4\pi}{3}\right)}_{\bar{P}_{ph}^{-+}}\end{aligned} \tag{3}$$

The main characteristic of the STATCOM application is that the positive- ($\cos\phi^+$) and negative-sequence power factors ($\cos\phi^-$) are zero (i.e., $\delta_v^+ \perp \theta_i^+$, and $\delta_v^- \perp \theta_i^-$). This means that there is not net energy transfer between the VSC and the application ($\bar{P}_\mathrm{a} + \bar{P}_\mathrm{b} + \bar{P}_\mathrm{c} = 0$).

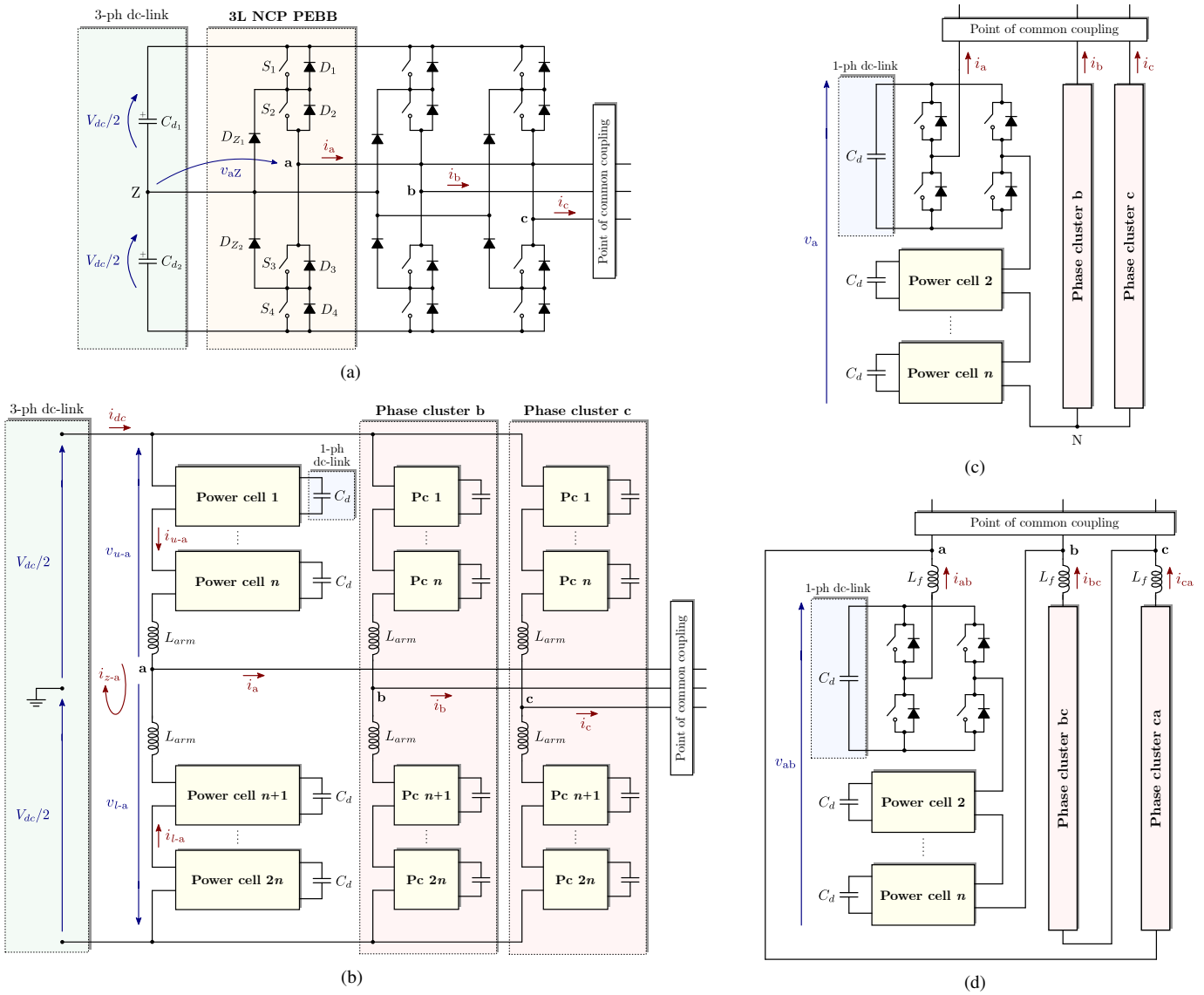

Fig. 1. Simplified circuit diagrams of the VSC structures under study. (a) 3L NPC, (b) MMC, (c) YCHB, and (d) DCHB.

In order to quantify the degree of current unbalance, the ratio k_{ipn} is defined [8]:

$$\text{for } I^+ \geq I^- \;\rightarrow\; k_{ipn} = \frac{I^-}{I^+} \;\rightarrow\; 0 \leq k_{ipn} \leq 1 \quad (4)$$

$$\text{for } I^+ \leq I^- \;\rightarrow\; k_{ipn} = 2 - \frac{I^+}{I^-} \;\rightarrow\; 1 \leq k_{ipn} \leq 2 \quad (5)$$

In addition to k_{ipn}, the angle between the current sequences ($\theta_{ipn} = \theta_i^- - \theta_i^+$) is another indicator which characterizes the current unbalance. Analogously, the ratio of voltage unbalance (k_{vpn}) can be defined [10]:

$$\text{for } V^+ \geq V^- \;\rightarrow\; k_{vpn} = \frac{V^-}{V^+} \;\rightarrow\; 0 \leq k_{vpn} \leq 1 \quad (6)$$

$$\text{for } V^+ \leq V^- \;\rightarrow\; k_{vpn} = 2 - \frac{V^+}{V^-} \;\rightarrow\; 1 \leq k_{vpn} \leq 2 \quad (7)$$

Sections IV and V analyze the impact of both the 2ω oscillating active power ($\tilde{p}$) and the average active power ($\bar{P}$) terms on the VSC STATCOM operating under v^- and/or i^-.

IV. Negative-Sequence Voltage and Current Effects on DC-Link Voltage Ripple

The oscillating active power term ($\tilde{p}$) has a zero average value and thus it does not represent any net energy exchange. However, as neglecting the inner losses of the converter the ac-side power should be equal to the dc-side, $\tilde{p}$ is responsible of the second-order harmonic (2ω) oscillation in the dc-link of the VSC. This oscillation generates a voltage ripple across the dc-link capacitor voltages (Δv_{dc}). As can be seen in (2), this effect depends on both the voltage and/or current unbalances, and on the dc-link configuration of the VSC. In order to quantify the dc voltage ripple, its peak-to peak value (Δv_{dc}^{pp}) is used as an indicator.

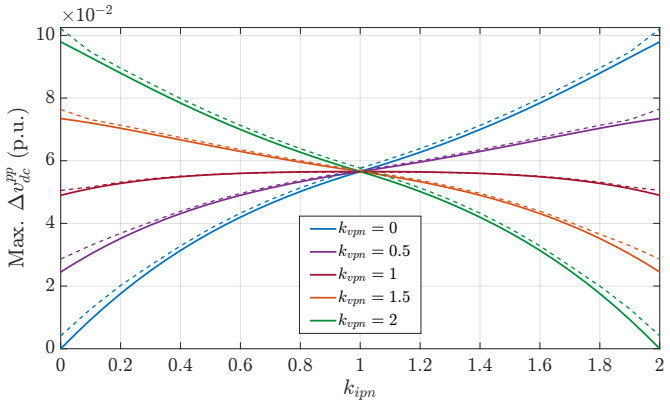

Fig. 2. Maximum dc-link voltage ripple peak-to-peak value of the 3L NPC STATCOM at rated voltage and current as a function of k_{ipn} for different k_{vpn} scenarios. Solid lines represent the analytical evolution, while the dashed ones show the time-based simulation results ($X_{C_{d_1}} = X_{C_{d_2}} = 0.13$ p.u.).

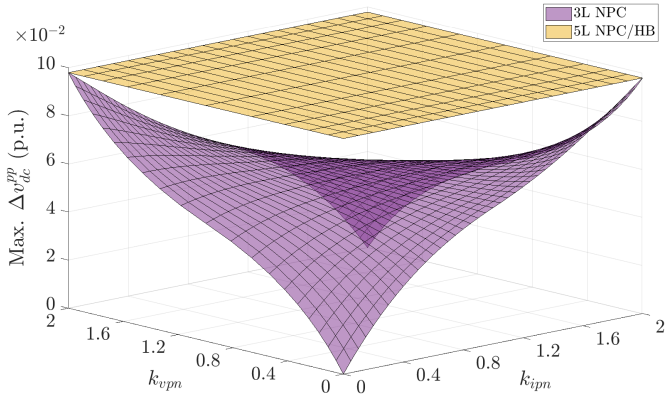

Fig. 3. Analytical maximum dc-link voltage ripple peak-to-peak value of the 3L NPC and 5L NPC/HB for STATCOM application at rated voltage and current as a function of k_{ipn} and k_{vpn} ($X_{C_{d\text{-}1\text{ph}}} = 2/3 \times X_{C_{d\text{-}3\text{ph}}}$).

When there is no cross-interaction between positive- and negative-sequences (only $\tilde{p}_{ph}^{++}$ or $\tilde{p}_{ph}^{--}$ exist), the three-phase oscillating active power is zero; i.e., the sum of $\tilde{p}_{ph}^{++}$ or $\tilde{p}_{ph}^{--}$ in the three phases is zero ($\tilde{p}_{\text{a}} + \tilde{p}_{\text{b}} + \tilde{p}_{\text{c}} = 0$). Hence, VSC structures with a three-phase dc-link such as the 3L NPC do not experience any dc voltage ripple under balanced conditions (at least not as a result of the 2ω oscillation), regardless the power factor (ϕ^+, ϕ^-) of the application. Nevertheless, while the presence of v^- and/ or i^- increases, the terms $\tilde{p}_{ph}^{+-}$ and/or $\tilde{p}_{ph}^{-+}$ arise in (2), which are common in the three phases. Thus, these terms do not cancel out when added together in the three phases, and are therefore responsible for creating a second-order harmonic voltage ripple in the three-phase dc-link.

With the aim of showing this effect, Fig. 2 shows the evolution of the maximum Δv_{dc}^{pp} of a 3L NPC for STATCOM application as a function of k_{ipn} (at the worst θ_{ipn} case), and for different k_{vpn} scenarios. The analytical results have been compared with time-based simulations. It can be seen how both results are very similar; the difference is the dc voltage ripple caused by the PWM switching harmonics, which has practically no weight compared to the dc voltage ripple caused by the cross-interaction between positive- and negative sequence-components. It is appreciated from Fig. 2 that the maximum Δv_{dc}^{pp} in a 3L NPC is given when uniquely $\tilde{p}_{ph}^{+-}$ or $\tilde{p}_{ph}^{-+}$ exist; that is, at operating points where all the voltage is positive-sequence ($k_{vpn} = 0$) and all the current negative ($k_{ipn} = 2$); as well as when all the voltage is negative-sequence ($k_{vpn} = 2$) and all the current positive ($k_{ipn} = 0$). This effect is clearly illustrated also in Fig. 3, where it is concluded that the current and voltage unbalances are analogous in their impact on the 2ω dc voltage ripple of a three-phase dc-link VSC. In a real application, if Δv_{dc}^{pp} increases, a current de-rating can be applied in order to decrease it; this would imply the de-rating of the available reactive power (Q) in the STATCOM, as it will be analyzed in Section VI. The dc-link capacitance (C_d) can also be over-rated so as to reduce this 2ω dc voltage ripple.

Regarding single-phase dc-link VSC structures, Fig. 3 presents also the evolution of Δv_{dc}^{pp} in a 5L NPC/HB STATCOM; which its maximum value is constant regardless k_{ipn} and k_{vpn}. That is, at rated voltage and current values, the maximum $\tilde{p}_{ph}$ of the three phase clusters is constant for any unbalance depth and type. Indeed, the maximum Δv_{dc}^{pp} in a single-phase dc-link VSC coincides with the maximum value of an equivalent three-phase dc-link VSC (considering the same C_d per PEBB), as can be deducted from (2).

Since there is no net energy exchange between the ac- and the dc-side, the physical three-phase dc energy-source can be avoided in the MMC for STATCOM application [15]. That means that the sum of the circulating dc currents in the three phases naturally sums up to zero ($i_{dc} = i_{z\text{-a}} + i_{z\text{-b}} + i_{z\text{-c}} = 0$). It should be noted that the oscillating active power ($\tilde{p}$) makes that the circulating current presents naturally a 2ω component, regardless of whether there are negative-sequences (v^-, i^-) or not. If the 2ω circulating current is neglected, the conclusions drawn about the impact of $\tilde{p}$ in Δv_{dc}^{pp} for single-phase dc-link VSCs are applied to the MMC.

In conclusion, VSC STATCOMs with single-phase dc-links do not present any limitation so as to deal with $\tilde{p}$ under unbalanced conditions, while a current de-rating must be applied to structures with a three-phase dc-link in order to withstand or inject v^- and/or i^-. Identical conclusions from Fig. 3 would be drawn if any equivalent single- and three-phase dc-link VSC structures were compared.

V. Negative-Sequence Voltage and Current Effects on Active Power Distribution

As mentioned, the main aspect of the STATCOM application is that there is no need of any energy-source, since, neglecting losses, the net active power exchange between the converter and the power grid is zero; i.e., $\bar{P}_{\text{a}} + \bar{P}_{\text{b}} + \bar{P}_{\text{c}} = 0$. From (3) it can be concluded that as long as there is no cross-interaction between positive- and negative-sequence components, the average active power which flows into each phase of the VSC STATCOM is also zero ($\bar{P}_{ph}^{++}$, $\bar{P}_{ph}^{--} = 0$). However, under unbalanced conditions terms $\bar{P}_{ph}^{+-}$ and/or $\bar{P}_{ph}^{-+}$ arise in

(3), which are also different in each phase cluster. This means that the phases of the VSC might deliver or absorb an active power different from zero ($\bar{P}_{\rm a} \neq \bar{P}_{\rm b} \neq \bar{P}_{\rm c} \neq 0$) [10].

Due to the fact that under unbalanced conditions the sum of $\bar{P}_{ph}^{+-}$ and/or $\bar{P}_{ph}^{-+}$ in the three phases is still zero ($\bar{P}_{\rm a} + \bar{P}_{\rm b} + \bar{P}_{\rm c} = 0$), structures with a three-phase dc-link do not need any dc energy-source for STATCOM application, whichever k_{vpn} and k_{ipn} are. This is the reason of removing the common three-phase dc-link in the MMC ($i_{dc} = 0$).

In contrast, the phase clusters of single-phase dc-link VSC structures might deliver or absorb an active power different from zero ($\bar{P}_{\rm a} \neq \bar{P}_{\rm b} \neq \bar{P}_{\rm c} \neq 0$) under unbalanced operation, even in STATCOM applications. The maximum $\bar{P}_{ph}$ is given when uniquely $\bar{P}_{ph}^{+-}$ or $\bar{P}_{ph}^{-+}$ exist; i.e., at $k_{vpn} = 0$ and $k_{ipn} = 2$, or at $k_{vpn} = 2$ and $k_{ipn} = 0$. As illustrated in Figs. 4 and 5, the current and voltage unbalances are analogous in their influence on the $\bar{P}_{ph}$ of a single-phase dc-link VSC.

The lack of a common three-phase dc-link involves that countermeasures must be taken in order to correct the uneven active power distribution between the phase clusters in single-phase dc-link VSCs for STATCOM application. Otherwise, dc-link voltage balancing cannot be guaranteed when operating with negative-sequences, and dc voltages might drift away from their rated levels. The adopted solution depends on the phase cluster connection configuration (YCHB or DCHB), and it might have an impact on the device power rating.

On the one hand, in case of the YCHB STATCOM, a fundamental-frequency common zero-sequence voltage (v_0) can be injected into the converter star point N [16], [17]. The addition of this component does not affect the three-phase voltages and currents at the PCC (see Fig. 6 (a)), and allows two degrees of freedom; its amplitude (V_0), and angle (δ_{v_0}):

$$v_0(t) = V_0 \sin(\omega t + \delta_{v_0}) \tag{8}$$

The aim is to find an appropriate V_0 and δ_{v_0} so as to generate an average active power term ($\bar{P}_{0\text{-}ph}^{\rm YCHB}$) which will cancel out the non-zero average active power at each phase cluster due to the cross-interaction between negative- and positive-sequence components ($\bar{P}_{ph}^{+-}$ and $\bar{P}_{ph}^{-+}$):

$$\begin{aligned}\bar{P}_{0\text{-}ph}^{\rm YCHB} &= \frac{V_0 I^+}{2} \cos\left(\delta_{v_0} - \theta_i^+ - k\frac{2\pi}{3}\right) \\ &+ \frac{V_0 I^-}{2} \cos\left(\delta_{v_0} - \theta_i^- + k\frac{2\pi}{3}\right) = -\bar{P}_{ph}^{+-} - \bar{P}_{ph}^{-+}\end{aligned} \tag{9}$$

Defining some constant terms (see Appendix A), the explicit expressions of δ_{v_0} and V_0 can be derived [17]:

$$\tan\delta_{v_0} = \frac{K_1^{\rm a}K_2^{\rm b} - K_1^{\rm b}K_2^{\rm a}}{K_1^{\rm b}K_3^{\rm a} - K_1^{\rm a}K_3^{\rm b}} \tag{10}$$

$$V_0 = \frac{-K_1^{ph}}{K_2^{ph}\cos\delta_{v_0} + K_3^{ph}\sin\delta_{v_0}} \tag{11}$$

Depending on k_{ipn} and k_{vpn}, the injection of v_0 could lead the converter voltage exceeding its rated level, and therefore resulting in the YCHB STATCOM operating in over-modulation or even becoming uncontrollable. That is, the zero-sequence voltage can be injected until the maximum attainable output voltage is reached. If this limit is reached, the converter can be over-rated either serializing more power cells or increasing the dc-link voltage.

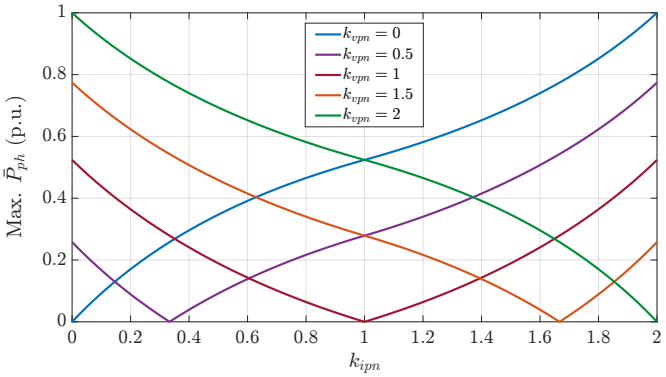

Fig. 4. Analytical maximum average active power of the 5L NPC/HB STATCOM at rated voltage and current as a function of k_{ipn} for different k_{vpn} scenarios.

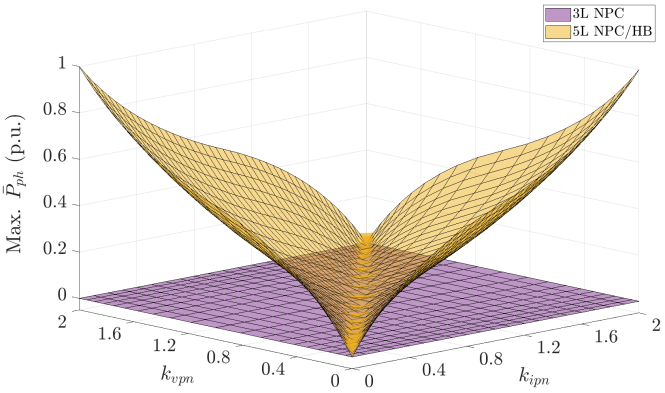

Fig. 5. Analytical maximum average active power of the 3L NPC and 5L NPC/HB for STATCOM application at rated voltage and current as a function of k_{ipn} and k_{vpn}.

On the other hand, if the DCHB is used for STATCOM, the delta configuration allows to correct the uneven active power distribution among the phase clusters by injecting a fundamental-frequency zero-sequence current (i_0) [16], [17]. As i_0 circulates only inside the delta, it does not affect the three-phase voltages and currents at the PCC (see Fig. 6 (b)). Similar to the YCHB, the injected i_0 allows two degrees of freedom, in terms of its amplitude (I_0), and angle (θ_{i_0}):

$$i_0(t) = I_0 \sin(\omega t + \theta_{i_0}) \tag{12}$$

The generated average active power ($\bar{P}_{0\text{-}ph}^{\rm DCHB}$) cancels out the terms $\bar{P}_{ph}^{+-}$ and $\bar{P}_{ph}^{-+}$:

$$\begin{aligned}\bar{P}_{0\text{-}ph}^{\rm DCHB} &= \frac{V^+ I_0}{2} \cos\left(\delta_v^+ - \theta_{i_0} + k\frac{2\pi}{3}\right) \\ &+ \frac{V^- I_0}{2} \cos\left(\delta_v^- - \theta_{i_0} - k\frac{2\pi}{3}\right) = -\bar{P}_{ph}^{+-} - \bar{P}_{ph}^{-+}\end{aligned} \tag{13}$$

being $k = 0, -1, 1$ for $ph = \mathrm{ab}, \mathrm{bc}, \mathrm{ca}$, respectively. Following the same criteria adopted for the YCHB (see Appendix B), θ_{i_0} and I_0 are calculated as [17]

$$\tan\theta_{i_0} = \frac{K_1^{\mathrm{ab}} K_2^{\mathrm{bc}} - K_1^{\mathrm{bc}} K_2^{\mathrm{ab}}}{K_1^{\mathrm{bc}} K_3^{\mathrm{ab}} - K_1^{\mathrm{ab}} K_3^{\mathrm{bc}}} \tag{14}$$

$$I_0 = \frac{-K_1^{ph}}{K_2^{ph}\cos\theta_{i_0} + K_3^{ph}\sin\theta_{i_0}} \tag{15}$$

The injected i_0 involves a current de-rating in the DCHB so as not to exceed the rated current of the switching devices. Thus, the available reactive power (Q) is reduced, as it is quantified in Section VI.

The average active power terms $\bar{P}_{ph}^{+-}$ and $\bar{P}_{ph}^{-+}$ are cancelled out also when added together in the three phase clusters of the MMC. Therefore, the energy-source connected to the common three-phase dc-link is also not needed to operate under v^- and/or i^- in STATCOM applications; i.e., $i_{dc} = 0$. However, the phase cluster active power differs from zero due to the cross-interaction between positive- and negative-sequence components. In order to redistribute the active power among the phase clusters, a dc current circulates in each phase cluster of the MMC $(i_{z\text{-}ph})$, and hence the charge of dc-link capacitors remains adjusted to the reference value in each phase cluster:

$$\bar{P}_{ph}^{+-} + \bar{P}_{ph}^{-+} = V_{dc} \cdot i_{z\text{-}ph} \tag{16}$$

Under balanced conditions $i_{z\text{-}ph}$ is zero, so the power cells are sized only considering the output ac current. But the appearance of this circulating dc current implies that a de-rating should be applied to the ac current so as not to exceed the rated current of the switching devices. This also means a reduction in the available Q.

In short, VSC structures with a common three-phase dc-link and without dc energy-sources do not require any solution to deal with i^- and/or v^- for STATCOM due to the uneven active power distribution. On the contrary, single-phase dc-links of CHBs will have to absorb or deliver active power even at STATCOM application, so will require a solution which will have an impact on the available reactive power. Regarding the MMC, the circulation of a dc current under unbalanced conditions will also limit the available Q of the device.

VI. Reactive Power Limits of the STATCOM under Unbalanced Voltage and/or Current Conditions

As seen in Sections IV and V, the presence of negative-sequence components $(v^-$ and/or $i^-)$ in STATCOM application has different effects depending on the dc-link configuration of the VSC. The countermeasures adopted so as to not exceeding the operational limits and remain connected to the PCC will have an impact on the power rating of the device. From the STATCOM manufacturer dimensioning point of view, the reactive power is the indicative parameter to define the most suitable VSC structure for a certain scenario. Accordingly, this section quantifies and compares the positive-sequence reactive power (Q^+) limits of the 3L NPC, YCHB, DCHB and MMC structures for STATCOM application operating with negative-sequence components $(v^-$ and/or $i^-)$. The output positive-sequence reactive power is defined as

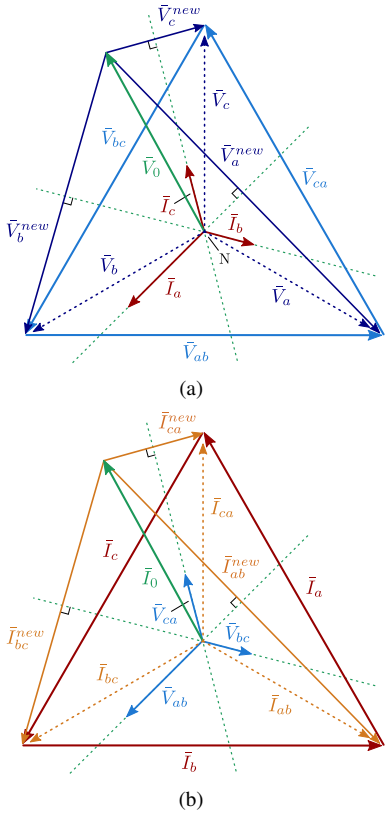

Fig. 6. Phasor diagrams of the fundamental-frequency zero-sequence (v_0 and i_0) injection. (a) YCHB under unbalanced current ($k_{ipn} > 0$, $k_{vpn} = 0$), and (b) DCHB under unbalanced voltage ($k_{vpn} > 0$, $k_{ipn} = 0$).

$$Q^+ = \frac{3}{2} V^+ I^+ \tag{17}$$

Figs. 7 (a) and (b) show the Q^+ limits of the VSCs under study for STATCOM application as a function of k_{ipn}. While in Fig. 7 (a) there is no voltage unbalance $(k_{vpn} = 0)$, in Fig. 7 (b) the ratio k_{vpn} is set to 0.15. These might be the typical scenarios of a STATCOM connected to the power grid, where v^- is null or very small in non-asymmetrical fault conditions (according to the corresponding grid code [11]).

The theoretical maximum attainable Q^+ in Fig. 7 refers to the inner product between v^+ and i^+ at rated values. This limit is achieved with a three-phase dc-link VSC such as the 3L NPC, sized in such a way (C_d) that the dc voltage ripple peak to peak (Δv_{dc}^{pp}) does not exceed the limit value; which is given in $k_{vpn} = 0$ and $k_{ipn} = 2$, or in $k_{vpn} = 2$ and $k_{ipn} = 0$ (see Fig. 3). If the three-phase dc-link is sized with a lower capacitance ($C_d/2$ or $C_d/4$ with dashed lines in Fig. 7), there is a k_{ipn} point at which the Δv_{dc}^{pp} limit is reached, and hence a de-rating must be applied to the current. As a result, the Q^+ limit begins to decrease (due to the reduction of i^+). This de-rating will be applied at lower k_{ipn} values as the dc-link capacitance is reduced.

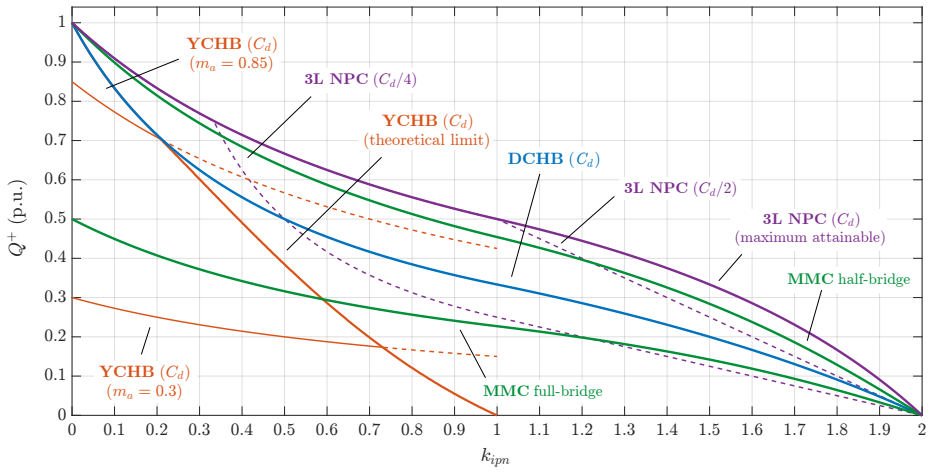

(a)

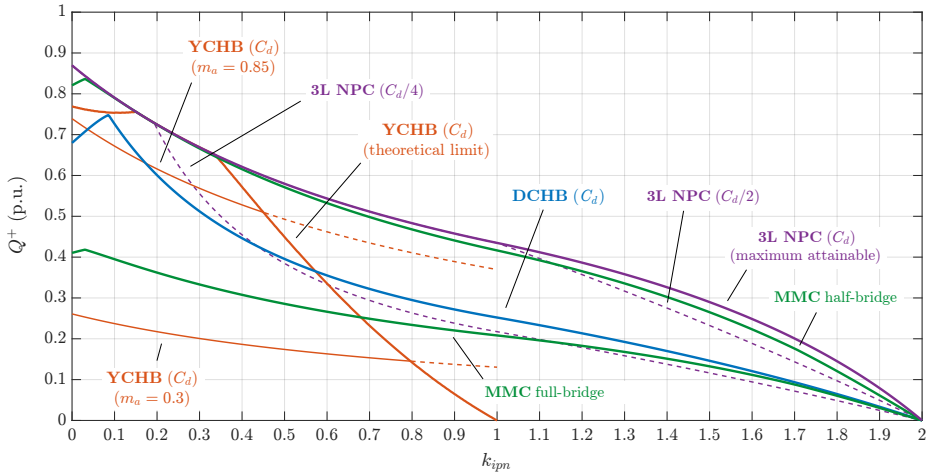

(b)

Fig. 7. Positive-sequence reactive power (Q^+) limits of YCHB (theoretical and real limits), DCHB, 3L NPC (for different dc-link capacitance values), and MMC (with full- and half-bridge power cells) for STATCOM application as a function of k_{ipn}. (a) $k_{vpn} = 0$, and (b) $k_{vpn} = 0.15$.

As mathematically seen, additional fundamental-frequency zero-sequence voltage (YCHB) or current (DCHB) are injected in CHB STATCOMs to deal with v^- and/or i^-, both of which vary depending on k_{ipn} and/or k_{vpn}. In this context, CHB structures will be limited in terms of voltage and/or current, depending on the circuit configuration.

The YCHB configuration cannot operate when the converter phase cluster voltage exceeds its rated level. Therefore, voltage over-rating is required so as to increase the available dc-side voltage. The plotted solid line in Fig. 7 illustrates the theoretical Q^+ limit of the correctly voltage over-rated YCHB for each k_{ipn}. This means that the converter is supposed to be able to give the reference voltage. In this configuration, the power de-rating is due to the i^+ decreasing as k_{ipn} increases (because i^- increases). As this voltage over-rating is not feasible in practice, limits for YCHB configurations with practical voltage ratings are also served (different amplitude modulation index values); dashed lines represent k_{ipn} operating points where the voltage limit is reached and the converter is not able to work. For instance, it can be seen that with $m_a = 0.85$ (which can be the case of a power grid-connected STATCOM), the YCHB cannot withstand a negative-sequence current up to $k_{ipn} = 0.2$ with $k_{vpn} = 0$, and up to $k_{ipn} = 0.45$ with $k_{vpn} = 0.15$. It can be seen that as v^- increases, the YCHB can operate under higher k_{ipn} values. An important drawback is that infinity V_0 is required in the operating point $k_{ipn} = 1$, regardless k_{vpn} [17]. That means that beyond this point, the YCHB becomes uncontrollable in practical applications. Thus, it can be concluded that the capability of the YCHB STATCOM to operate under negative-sequences is strongly limited by the voltage rating of its phase clusters, as well as it is more vulnerable to current unbalance than voltage unbalance.

With regard to the DCHB, the line plotted in Fig. 7 decreases when k_{ipn} increases either as a result of the phase cluster i^+ de-rating due to the increasing of i_0, and/or the decreasing of i^+ as i^- increases. As stated above, and in contrast with the YCHB, the delta configuration does not present any limitation in terms of exceeding the rated voltage. That is why it can ensure the controllability of dc-link capacitor voltages guaranteeing the nominal ac voltage of the PCC up

to $k_{ipn} = 2$, as the grid code might demand. This is the major advantage of the delta over the star. However, as it can be seen in Fig. 7, the DCHB is more vulnerable to the voltage unbalance. Besides, it requires infinity I_0 in the operating point $k_{vpn} = 1$. At this singular point the converter becomes uncontrollable, and dc-link voltages would drift away; this is the only operating condition where the DCHB cannot operate. As demonstrated in [17], a duality exists between the voltage rating of the YCHB under unbalanced current conditions, and the current rating of the DCHB under unbalanced voltage conditions. However, it is noteworthy that the condition of singularity for the DCHB ($k_{vpn} = 1$) is less likely to occur in practice than the condition for the YCHB ($k_{ipn} = 1$), which makes the delta configuration more interesting for STATCOM applications and negative-sequence injection.

Finally, both half-bridge and full-bridge configured MMC structures are shown in Fig. 7. The Q^+ limit of both configurations decrease when k_{ipn} increases due to the i^+ de-rating as a result of the increasing of the circulating dc current $i_{z\text{-}ph}$. That is to say, the difference between the maximum attainable Q^+ limit and the half-bridge MMC Q^+ limit is due to the dc current which circulates in each phase cluster of the MMC. Since the number of installed semiconductor devices is two times higher in the full-bridge than in the half-bridge, the Q^+ limit is reduced by half. However, the redundancy and the fault tolerance are enhanced when using full-bridge power cells.

VII. Conclusion

Negative-sequence operation implies that new terms appear in both the second-order harmonic oscillating and the average active power terms. These terms have an effect on the dc-link voltage ripple of three-phase dc-link VSCs, and on the uneven active power distribution in single-phase dc-link VSCs.

This paper has analyzed the impact of negative-sequence components on the reactive power limits of a STATCOM. The raised conclusions are extendable to any PEBB topology used in each VSC structure.

Acknowledgment

This work has been partially funded by a predoctoral grant (FPU18/04246) and a research grant (GASAC RTC-2017-26091-3) from the Spanish Government.

Appendix

A. Constant terms for the calculation of v_0 in the YCHB

Being $k = 0, -1, 1$ for $ph = \mathrm{a}, \mathrm{b}, \mathrm{c}$, respectively:

$$\begin{aligned} K_1^{ph} &= V^+ I^- \cos\left(\delta_v^+ - \theta_i^- + k\frac{4\pi}{3}\right) \\ &\quad + V^- I^+ \cos\left(\delta_v^- - \theta_i^+ - k\frac{4\pi}{3}\right) \\ K_2^{ph} &= I^+ \cos\left(\theta_i^+ + k\frac{2\pi}{3}\right) + I^- \cos\left(\theta_i^- - k\frac{2\pi}{3}\right) \\ K_3^{ph} &= I^+ \sin\left(\theta_i^+ + k\frac{2\pi}{3}\right) + I^- \sin\left(\theta_i^- - k\frac{2\pi}{3}\right) \end{aligned} \tag{18}$$

B. Constant terms for the calculation of i_0 in the DCHB

Being $k = 0, -1, 1$ for $ph = \mathrm{ab}, \mathrm{bc}, \mathrm{ca}$, respectively:

$$\begin{aligned} K_1^{ph} &= V^+ I^- \cos\left(\delta_v^+ - \theta_i^- + k\frac{4\pi}{3}\right) \\ &\quad + V^- I^+ \cos\left(\delta_v^- - \theta_i^+ - k\frac{4\pi}{3}\right) \\ K_2^{ph} &= V^+ \cos\left(\delta_v^+ + k\frac{2\pi}{3}\right) + V^- \cos\left(\delta_v^- - k\frac{2\pi}{3}\right) \\ K_3^{ph} &= V^+ \sin\left(\delta_v^+ + k\frac{2\pi}{3}\right) + V^- \sin\left(\delta_v^- - k\frac{2\pi}{3}\right) \end{aligned} \tag{19}$$

References

[1] J. M. Carrasco *et al.*, "Power-electronic systems for the grid integration of renewable energy sources: a survey," *IEEE Trans. Ind. Electron.*, vol. 53, no. 4, pp. 1002–1016, 2006.

[2] B. K. Bose, "Power electronics and motor drives recent progress and perspective," *IEEE Trans. Ind. Electron.*, vol. 56, no. 2, pp. 581–588, 2009.

[3] S. Kouro *et al.*, "Recent advances and industrial applications of multilevel converters," *IEEE Trans. Ind. Electron.*, vol. 57, no. 8, pp. 2553–2580, 2010.

[4] T. Tanaka, K. Ma, H. Wang, and F. Blaabjerg, "Asymmetrical reactive power capability of modular multilevel cascade converter based STATCOMs for offshore wind farm," *IEEE Trans. Power Electron.*, vol. 34, no. 6, pp. 5147–5164, 2019.

[5] H. Akagi, "Classification, terminology, and application of the modular multilevel cascade converter (MMCC)," *IEEE Trans. Power Electron.*, vol. 26, no. 11, pp. 3119–3130, 2011.

[6] D. Soto and T. C. Green, "A comparison of high-power converter topologies for the implementation of FACTS controllers," *IEEE Trans. Ind. Electron.*, vol. 49, no. 5, pp. 1072–1080, 2002.

[7] A. Nabae, I. Takahashi, and H. Akagi, "A new neutral-point-clamped PWM inverter," *IEEE Trans. Ind. Appl.*, vol. IA-17, no. 5, pp. 518–523, 1981.

[8] I. Marzo, J. A. Barrena, and A. Sanchez-Ruiz, "Methodology to evaluate converter structures based on 3L NPC PEBBs," in *IECON 2020 - 46th Annu. Conf. IEEE Ind. Electron. Soc.*, pp. 4107–4114, 2020.

[9] M. Malinowski, K. Gopakumar, J. Rodriguez, and M. A. Perez, "A survey on cascaded multilevel inverters," *IEEE Trans. Ind. Electron.*, vol. 57, no. 7, pp. 2197–2206, 2010.

[10] I. Marzo, A. Sanchez-Ruiz, J. A. Barrena, G. Abad, and I. Muguruza, "Power balancing in cascaded H-bridge and modular multilevel converters under unbalanced operation: A review," *IEEE Access*, vol. 9, pp. 110 525–110 543, 2021.

[11] IEC 61000-2-4, "Electromagnetic compatibility (EMC) – Part 2-4: Environment - Compatibility levels in industrial plants for low-frequency conducted disturbances," 2004.

[12] Verband der Elektrotechnik Elektronik Informationstechnik (VDE), "Technical Connection Rules for High-Voltage (VDE-AR-N 4120)," 2018.

[13] P. W. Hammond, "A new approach to enhance power quality for medium voltage AC drives," *IEEE Trans. Ind. Appl.*, vol. 33, no. 1, pp. 202–208, 1997.

[14] A. Lesnicar and R. Marquardt, "An innovative modular multilevel converter topology suitable for a wide power range," in *2003 IEEE Bol. PowerTech Conf.*, pp. 1–6, 2003.

[15] A. F. Cupertino, J. V. M. Farias, H. A. Pereira, S. I. Seleme, and R. Teodorescu, "Comparison of DSCC and SDBC modular multilevel converters for STATCOM application during negative sequence compensation," *IEEE Trans. Ind. Electron.*, vol. 66, no. 3, pp. 2302–2312, 2019.

[16] R. E. Betz, T. Summers, and T. Furney, "Symmetry compensation using a H-bridge multilevel STATCOM with zero sequence injection," in *41st IAS Annu. Meet. Conf. Rec. 2006 Ind. Appl. Conf.*, pp. 1724–1731, 2006.

[17] E. Behrouzian and M. Bongiorno, "Investigation of negative-sequence injection capability of cascaded H-bridge converters in star and delta configuration," *IEEE Trans. Power Electron.*, vol. 32, no. 2, pp. 1675–1683, 2017.